Phonon-Limited Transport in Graphene Pseudospintronic Devices

Z. J. Estrada, B. Dellabetta, U. Ravaioli, and M. J. Gilbert

***Abstract*—A predicted room-temperature phase transition from Fermi liquid to dissipationless Bose–Einstein exciton superfluid suggests that graphene pseudospin devices may have the potential to far outperform traditional CMOS devices. When examining the possibility of a room-temperature exciton condensate, it is important to consider scattering of charge carriers by phonons in each of the constituent graphene monolayers. Using the nonequilibrium Green's function formalism, we examine the effect that carrier-phonon scattering has on device performance. We find that the effect of carrier-phonon scattering has strong dependence on the device coherence length. As such, for large gate voltages, the effect of phonons on interlayer transport is negligible.**

***Index Terms*—Critical current, nanoelectronics, phonons, tunneling.**

IT IS generally accepted that MOSFET scaling cannot continue unabated. In light of this, one of the most active areas of semiconductor electronics research is post-CMOS device technology. A variety of post-CMOS devices are under active consideration. In an effort to reach the smallest possible dimensions, molecular electronics has gained serious attention. While molecular electronics offers high device density and low-power operation, issues surrounding the molecule–electrode coupling, low yield, and three-terminal device fabrication [1] plague development. Improvements in nanoscale fabrication techniques have sparked interest in replacing CMOS with nanoelectromechanical systems (NEMSs). NEMSs offer small leakage current and a large on–off ratio [2]; however, high-frequency switching speed and reliability remain unsolved challenges. Beyond these relatively exotic solutions, the tunnel field-effect transistor (TFET), whose operation is based on band-to-band tunneling [3], has shown much recent progress. TFETs showcase a low OFF-state current and a subthreshold slope experimentally demonstrated to be less than 60 mV/dec for carbon nanotube TFETs. However, TFETs also possess a low ON-state current, which must be significantly improved if these devices are to be implemented in information processing technologies.

Manuscript received June 5, 2012; revised June 26, 2012; accepted June 30, 2012. Date of publication August 6, 2012; date of current version September 21, 2012. This work was supported by the Army Research Office under Contract W911NF-09-1-0347. The review of this letter was arranged by Editor Z. Chen.

Z. J. Estrada, B. Dellabetta, and M. J. Gilbert are with the Department of Electrical and Computer Engineering and Micro and Nanotechnology Laboratory, University of Illinois, Urbana-Champaign, Urbana, IL 61801 USA (e-mail: zestrad2@illinois.edu).

U. Ravaioli is with the Department of Electrical and Computer Engineering and Beckman Institute, University of Illinois, Urbana-Champaign, Urbana, IL 61801 USA.

Color versions of one or more of the figures in this letter are available online at http://ieeexplore.ieee.org.

Digital Object Identifier 10.1109/LED.2012.2207701

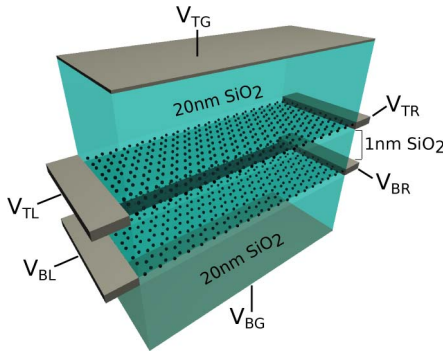

Fig. 1. Schematic of the device under consideration in this letter. Here, we have two monolayers of graphene separated by 1 nm of SiO_2. Each layer has a separate set of contacts (V_{TL} and V_{TR} for the top layer and V_{BL} and V_{BR} for the bottom layer) from which current may be injected and extracted. Top and bottom gates, i.e., V_{TG} and V_{BG}, are used to adjust the layer carrier concentrations.

Graphene-based pseudospintronic (G-PsS) devices are predicted to exhibit a high ON-state current with low-power dissipation [4]–[6]. It has been proposed that G-PsS devices could outperform traditional CMOS as they operate based on coherent interlayer transport rather than on the principle of source injected charge based on thermionic emission. In some works, graphene-based pseudospin devices have been predicted to possess a room-temperature phase transition from normal Fermi liquid behavior to a Bose–Einstein condensate of indirectly bound excitons formed when electrons present in one layer bind with an equal number of holes in the other layer [7]–[9]. The transition temperature has not been theoretically resolved [10], and other works predict an orders-of-magnitude lower transition temperature [11]. Still, recent Coulomb drag experiments have provided evidence of the interlayer interactions which may lead to the experimental realization of an exciton condensate in a double-layer graphene [12]. The formation of an interlayer coherent state allows for ultralow power operation as we may switch the device from on to off simply by shifting the energy of the ensemble of charge rather than shifting each charge itself. The operation of such a device at room temperature necessitates the examination of the electron–phonon interaction between the constituent quasi-particles and relevant phonon modes [13]. In this letter, we investigate the effects of the electron–phonon interaction on the room-temperature G-PsS device operation. We find that, at large gate voltages, the effects of phonon interactions become negligible due to the short coherence length in G-PsS devices. While at lower gate voltages, G-PsS device transport properties are significantly degraded by the phonon interaction.

In Fig. 1, we show a schematic of the graphene pseudospin device that we consider in this letter. The proposed device

is composed of two monolayers of graphene with lengths of 30 nm and widths of 10 nm. The layers are considered to be perfectly registered ideal sheets of zigzag graphene, such that the lattice sites of each layer are aligned. Each monolayer is terminated with an independent set of metal contacts from which current may be injected and extracted. We assume an ideal model for these contacts, which do not cause unintentional doping of the graphene layers [14]. The graphene monolayers are separated by a 1-nm layer of SiO_2, which serves as a tunnel dielectric with a corresponding single-particle tunneling amplitude of $\Delta_{\rm sas} = 1$ μeV. Each layer is individually gated to independently control the layer carrier concentrations with the gates separated from the layers by 20 nm of SiO_2. In order to most effectively drive the interlayer condensate current, we apply the bias voltage in the drag–counterflow configuration [15] in which a positive interlayer voltage is applied to the top left contact $V_{\rm TL}$ and an equal negative interlayer bias is applied to the top right contact $V_{\rm TR}$ while the contacts in the bottom layer remain grounded ($V_{\rm BL} = V_{\rm BR} = 0$ V). The interlayer current discussed here is then measured flowing from the top left contact to the bottom left contact.

To model our system, we use a tight-binding Hamiltonian to represent each of the layers

$$H_{\rm layer} = \sum_{<i,j>} \tau |i\rangle\langle j| + V_i |i\rangle\langle i| \tag{1}$$

where lattice points i and j are the first nearest neighbors. $\tau = -3.03$ eV is the nearest neighbor hopping energy for the p_z orbital of graphene, which allows for the unique low-energy linear dispersion at the K and K' points in the Brillouin zone. The full system Hamiltonian is formed as

$$\mathcal{H}_{\rm sys} = \begin{bmatrix} H_{\rm layer} & 0 \\ 0 & H_{\rm layer} \end{bmatrix} + \sum_{\mu=x,y,z} \hat{\mu} \cdot \vec{\Delta} \otimes \sigma_\mu \tag{2}$$

with the interlayer interactions, including both single-particle tunneling and mean-field many-body contribution $\vec{\Delta}$, coupling the two layers using a local density approximation, which drives the phase transition [16]. In (2), μ represents a vector that isolates each of the Cartesian components of the pairing vector, and σ_μ represents the Pauli spin matrices in each of the three spatial directions. On-site potential energy V_i is calculated via a 3-D Poisson solver. The transport quantities are calculated via the nonequilibrium Green's function (NEGF) formalism [17] self-consistently with the interlayer interactions and the electrostatics. We introduce carrier-phonon scattering to our Hamiltonian within the self-consistent Born approximation [18]. We include the relevant self-energy terms for both elastic acoustic phonon scattering (with deformation potential $D_{\rm ac} = 19$ eV) [19] and inelastic optical phonon scattering processes (with optical deformation potential $D_{\rm op} = 1 \times 10^9$ eV/cm and energy $\hbar\omega_0 = 164.6$ meV) [20], in which both interband and intraband scattering are included by utilizing a real-space basis [21]. We have set the system temperature to be $T_{\rm sys} = 300$ K for all calculations.

In G-PsS devices, the most important parameter to device performance is critical current I_c or the maximum interlayer current that the system can sustain by adjusting the interlayer phase relationship. I_c is defined as [22]

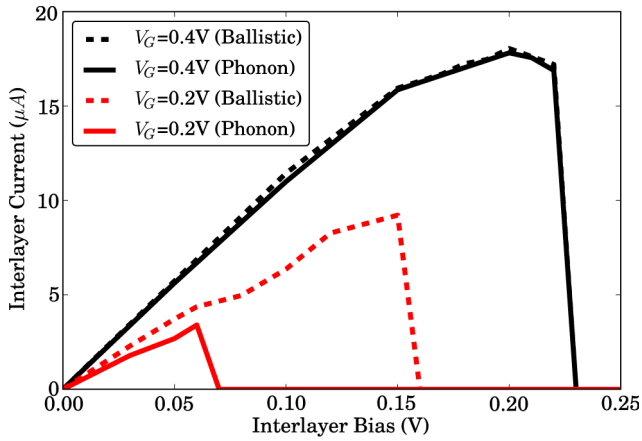

Fig. 2. Current–voltage characteristic obtained from NEGF simulations comparing (dotted lines) ballistic and (solid lines) phonon cases for two gate voltages, (black) $V_G = 0.4$ V and (red) $V_G = 0.2$ V.

$$I_c \sim \frac{qW\rho_s}{\hbar L_c}. \tag{3}$$

In (3), q is the electronic charge, W is the width of the system, ρ_s is the pseudospin phase stiffness, and L_c is the coherence length. The coherence length in pseudospin systems expected to form a condensate phase defines the maximum length which quasi-particles propagate in the system before undergoing retroreflection. When a quasi-particle is retroreflected, the system launches an exciton to conserve current [5]. The process is similar to Andreev reflections in a superconductor, except that here electrons are injected in one layer and are reflected as electrons with opposite momentum in the other layer. The coherence length is inversely proportional to the Fermi wavenumber k_F and is approximately given by [5]

$$L_c \sim \frac{1}{k_F}\sqrt{\frac{\rho_s}{\Delta_{\rm sas}}}. \tag{4}$$

The critical current is defined as the maximum interlayer current attained before self-consistency is lost. After the system passes the interlayer voltage corresponding to the critical current, the interlayer current plummets as the system can no longer sustain the condensate phase and interlayer tunneling becomes dominated by single-particle tunneling [16], [23]. We plot the interlayer current–voltage characteristic calculated for two values of gate voltage in Fig. 2. We first examine the critical current with a gate voltage of $V_{\rm TG} = -V_{\rm BG}$ (hereafter referred to as V_G) $= 0.40$ V, a value chosen to place the system well within the predicted regime for room-temperature superfluidity [8]. We find that the critical current for the ballistic case is $I_c \approx 18.4$ μA, in good agreement with the analytic value of $I_c^A \approx 19.5$ μA, whereas $I_c^{\rm ph} \approx 17.9$ μA when the phonon interactions are included representing a change of only 2.7%. At $V_G = 0.20$ V, we find a critical current of $I_c \approx 10.0$ μA for the ballistic case, and $I_c^{\rm ph} \approx 3.4$ μA when phonon interactions are included, a 66.0% drop in critical current.

To better illustrate the role of phonons in graphene pseudospin device operation, we plot the critical current considering both the ballistic and phonon interaction cases versus V_G in Fig. 3. Gate voltages below 0.20 V are outside of the predicted

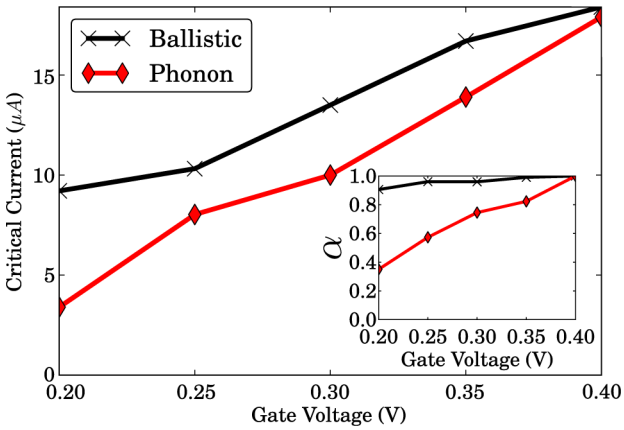

Fig. 3. Value of critical current I_c found at different values of gate voltage V_G for both (black) the ballistic case and (red) the phonon-limited case. (Inset) Plot of the average self-consistent value of ρ_s normalized to ρ_s at $V_G = 0.4$ V ($\alpha = \rho_s/\rho_s(V_G = 0.4\text{ V})$) with and without phonon interactions.

regime of room-temperature condensation, and values above 0.40 V require fields approaching the dielectric breakdown potential of SiO_2. Critical current in the ballistic case linearly decreases with Fermi energy due to the linear dependence of both I_c and E_F on k_F.

However, simple changes in L_c are insufficient to explain the observed drop in I_c with decreasing V_G seen when considering phonon interactions. While it is true that L_c does linearly decrease with decreasing V_G in the ballistic case, this is untrue when phonon interactions are considered. To explain the nonlinear drop in critical current seen when phonon interactions are considered, we plot the average self-consistent value of ρ_s normalized to ρ_s at $V_G = 0.4$ V for our device with and without phonon interactions in the inset of Fig. 3. For the ballistic case, we see that ρ_s remains close to unity deviating at lower V_G due to confinement effects. Nevertheless, we see that when phonons are included, ρ_s quickly drops as V_G decreases. This is due to the fact that quasi-particles can penetrate farther into the device before being retroreflected. This leads to carriers interacting with the phonons in the individual graphene layers more strongly. The energy changes in the carriers due to scattering serve to energetically separate the excitons prematurely breaking interlayer coherence and leading to a large drop in the value of ρ_s and the corresponding drop in I_c as V_G decreases in the presence of phonons.

In conclusion, we have performed quantum transport simulations to study the impact of carrier-phonon scattering on device performance in G-PsS devices. We observe that the effect of phonon scattering on the critical current depends in an intricate way on both the value of the coherence length and the pseudospin phase stiffness of the system. At short coherence lengths, which occur at high gate voltages, we find that the critical current is not affected by the presence of phonon interactions. However, at lower gate voltages, the critical current is significantly reduced by the presence of phonon interactions. This places limits on the operational gate voltages, which should be used in conjunction with G-PsS devices to achieve maximum device performance.

ACKNOWLEDGMENT

Z. J. Estrada would like to thank D. E. Nikonov, Y. Yoon, and S. Salahuddin for many insightful discussions. The authors would like to thank the Center for Scientific Computing from the CNSI at the University of California, Santa Barbara, MRL for computational support: an NSF MRSEC (DMR-1121053), Hewlett-Packard, and NSF CNS-0960316.

REFERENCES

[1] D. Vuillaume, "Molecular nanoelectronics," *Proc. IEEE*, vol. 98, no. 12, pp. 2111–2123, Dec. 2010.
[2] V. Pott, H. Kam, R. Nathanael, J. Jeon, E. Alon, and T. K. Liu, "Mechanical computing redux: Relays for integrated circuit applications," *Proc. IEEE*, vol. 98, no. 12, pp. 2076–2094, Dec. 2010.
[3] A. M. Ionescu and H. Riel, "Tunnel field-effect transistors as energy-efficient electronic switches," *Nature*, vol. 479, no. 7373, pp. 329–337, Nov. 2011.
[4] S. K. Banerjee, L. F. Register, E. Tutuc, D. Reddy, and A. H. MacDonald, "Bilayer pseudospin field-effect transistor (BiSFET): A proposed new logic device," *IEEE Electron Device Lett.*, vol. 30, no. 2, pp. 158–160, Feb. 2009.
[5] M. J. Gilbert, "Performance characteristics of scaled bilayer graphene pseudospin devices," *IEEE Trans. Electron Devices*, vol. 57, no. 11, pp. 3059–3067, Nov. 2010.
[6] K. Bernstein, R. K. Cavin, W. Porod, A. Seabaugh, and J. Welser, "Device and architecture outlook for beyond CMOS switches," *Proc. IEEE*, vol. 98, no. 12, pp. 2169–2184, Dec. 2010.
[7] M. J. Gilbert and J. Shumway, "Probing quantum coherent states in bilayer graphene," *J. Comput. Electron.*, vol. 8, no. 2, pp. 51–59, Jun. 2009.
[8] H. Min, R. Bistritzer, J. Su, and A. H. MacDonald, "Room-temperature superfluidity in graphene bilayers," *Phys. Rev. B*, vol. 78, no. 12, pp. 121401-1–121401-4, Sep. 2008.
[9] C. Zhang and Y. N. Joglekar, "Excitonic condensation of massless fermions in graphene bilayers," *Phys. Rev. B*, vol. 77, no. 23, pp. 233405-1–233405-4, Jun. 2008.
[10] J. Shumway and M. J. Gilbert, "Effects of fermion flavor on exciton condensation in double-layer systems," *Phys. Rev. B*, vol. 85, no. 3, pp. 033103-1–033103-4, Jan. 2012.
[11] M. Y. Kharitonov and K. B. Efetov, "Excitonic condensation in a double-layer graphene system," *Semicond. Sci. Technol.*, vol. 25, no. 3, p. 034004, Mar. 2010.
[12] S. Kim, I. Jo, J. Nah, Z. Yao, S. K. Banerjee, and E. Tutuc, "Coulomb drag of massless fermions in graphene," *Phys. Rev.*, vol. 83, no. 16, pp. 161401-1–161401-4, Apr. 2011.
[13] A. Akturk and N. Goldsman, "Electron transport and full-band electron-phonon interactions in graphene," *J. Appl. Phys.*, vol. 103, no. 5, pp. 053702-1–053702-8, Mar. 2008.
[14] J. Cayssol, B. Huard, and D. Goldhaber-Gordon, "Contact resistance and shot noise in graphene transistors," *Phys. Rev. B*, vol. 79, no. 7, pp. 075428-1–075428-6, Feb. 2009.
[15] J. Su and A. H. MacDonald, "How to make a bilayer exciton condensate flow," *Nat. Phys.*, vol. 4, no. 10, pp. 799–802, Oct. 2008.
[16] M. J. Gilbert, "Finite-temperature pseudospin torque effect in graphene bilayers," *Phys. Rev. B*, vol. 82, no. 16, pp. 165408-1–165408-12, Oct. 2010.
[17] S. Datta, *Quantum Transport: Atom to Transistor*. Cambridge, U.K.: Cambridge Univ. Press, 2005.
[18] D. Nikonov, H. Pal, and G. Bourianoff, *Scattering in NEGF: Made simple*, Nov. 2009. [Online]. Available: http://nanohub.org/resources/7772
[19] E. H. Hwang and S. Das Sarma, "Acoustic phonon scattering limited carrier mobility in two-dimensional extrinsic graphene," *Phys. Rev. B*, vol. 77, no. 11, pp. 115449-1–115449-6, Mar. 2008.
[20] K. M. Borysenko, J. T. Mullen, E. A. Barry, S. Paul, Y. G. Semenov, J. M. Zavada, M. B. Nardelli, and K. W. Kim, "First-principles analysis of electron-phonon interactions in graphene," *Phys. Rev. B*, vol. 81, no. 12, pp. 121412-1–121412-4, Mar. 2010.
[21] Y. Yoon, D. E. Nikonov, and S. Salahuddin, "Role of phonon scattering in graphene nanoribbon transistors: Nonequilibrium greens function method with real space approach," *Appl. Phys. Lett.*, vol. 98, no. 20, pp. 203503-1–203503-3, May 2011.
[22] J. Su and A. H. MacDonald, "Critical tunneling currents in quantum hall superfluids: Pseudospin-transfer torque theory," *Phys. Rev. B*, vol. 81, no. 18, pp. 184523-1–184523-11, May 2010.
[23] B. Dellabetta and M. J. Gilbert, "The effect of disorder in superfluid double layer graphene," *J. Phys., Condens. Matter*, vol. 23, pp. 345302-1–345302-11, Aug. 2011.